Cell Reports, Volume *32*

Supplemental Information

Single-Cell and Population Transcriptomics Reveal Pan-epithelial Remodeling in Type 2-High Asthma

Nathan D. Jackson, Jamie L. Everman, Maurizio Chioccioli, Luigi Feriani, Katherine C. Goldfarbmuren, Satria P. Sajuthi, Cydney L. Rios, Roger Powell, Michael Armstrong, Joe Gomez, Cole Michel, Celeste Eng, Sam S. Oh, Jose Rodriguez-Santana, Pietro Cicuta, Nichole Reisdorph, Esteban G. Burchard, and Max A. Seibold

Figure S1

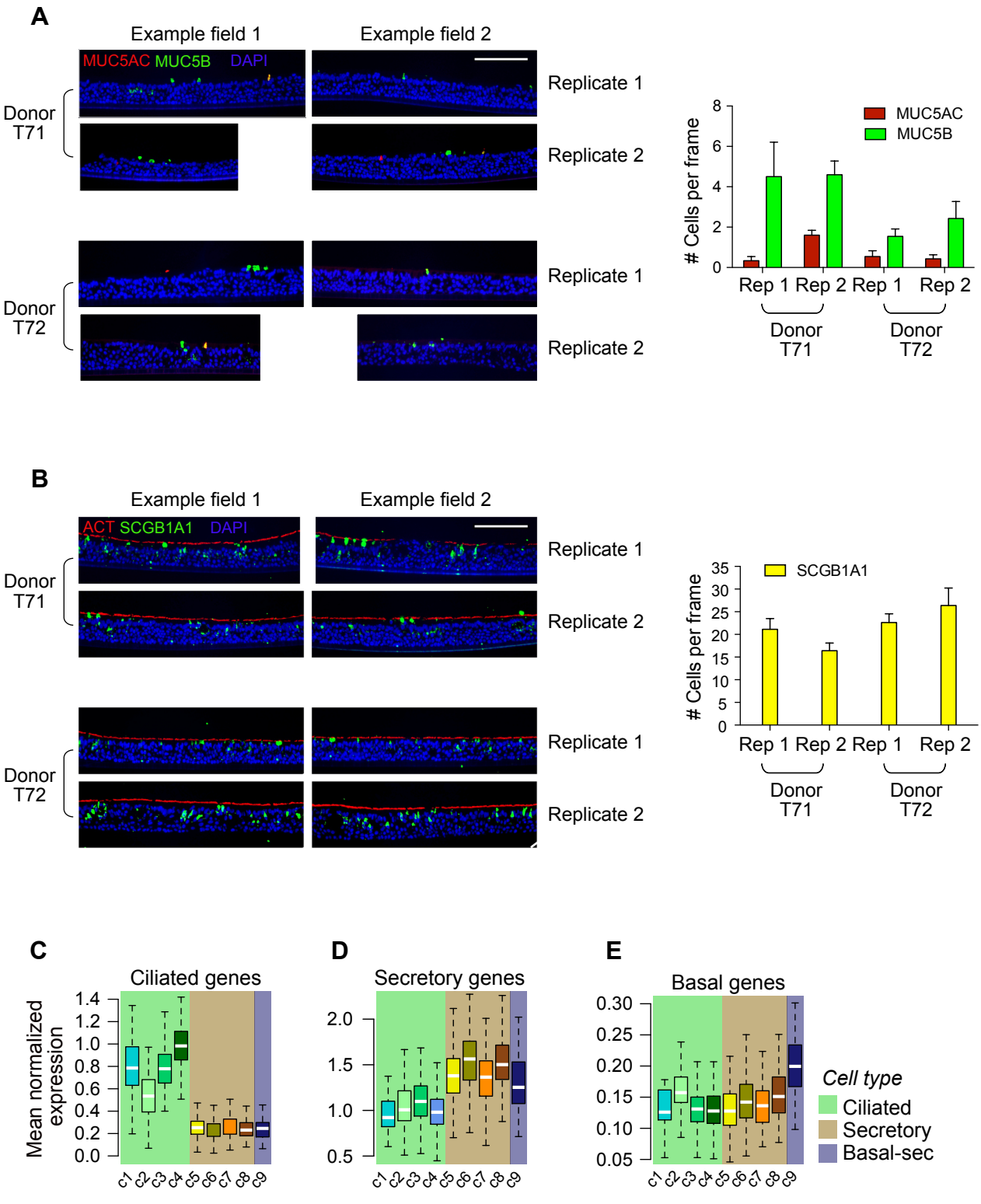
A
Example field 1
Example field 2
MUC5AC MUC5B DAPI
Donor T71
Donor T72
Replicate 1
Replicate 2
Cells per frame
MUC5AC
MUC5B
Rep 1 Rep 2 Rep 1 Rep 2
Donor T71
Donor T72
B
ACT SCGB1A1 DAPI
SCGB1A1
C
Ciliated genes
Mean normalized expression
D
Secretory genes
E
Basal genes
Cell type
Ciliated
Secretory
Basal-sec

Figure S1 (related to Figure 2). Characterization of cell types in the human airway epithelium *in vitro*
(A) *Left*, Immunofluorescence (IF) labeling of ALI-differentiated human AEC cultures in profile views show prevalence of $MUC5AC^+$ (red) and $MUC5B^+$ (green) cells in two replicate inserts for the two HTEC donors used for scRNA-seq. Two example fields are shown for each replicate. Scale bar = 130 μm; DAPI labeling of nuclei (blue). *Right*, IF quantification of $MUC5AC^+$ and $MUC5B^+$ cells across multiple fields for each replicate (N fields, from left to right = 6, 6, 11, 7). Bars give the mean number of cells across fields and error bars give standard error.
(B) *Left*, Immunofluorescence (IF) labeling of ALI-differentiated human AEC cultures in profile views show prevalence of $SCGB1A1^+$ (green) cells in two replicate inserts for the two HTEC donors used for scRNA-seq. Two example fields are shown for each replicate. Scale bar = 130 μm; ACT labeling (red) and DAPI labeling of nuclei (blue). *Right*, IF quantification of $SCGB1A1^+$ cells across multiple fields for each replicate (N fields, from left to right = 8, 5, 8, 8). Bars give mean number of cells across fields and error bars give standard error.
(C) Box plots of mean expression for ciliated cell signature genes across unsupervised clusters show that ciliated cell genes reach their highest expression in clusters c1 – c4. Expression in these four clusters is significantly higher than in each of the other clusters based on one-sided Wilcoxon signed-rank tests (p-value < 0.05).
(D) Box plots of mean expression for secretory signature genes across unsupervised clusters show that secretory genes reach their highest expression in clusters c5 – c9, Expression in these five clusters is significantly higher than in each of the other clusters based on one-sided Wilcoxon signed-rank tests (p-value < 0.05).
(E) Box plots of mean expression for basal cell signature genes across unsupervised clusters show that basal cell genes are uniquely characteristic of c9. Expression in c9 is significantly higher than in each of the other clusters based on one-sided Wilcoxon signed-rank tests (p-value < 0.05).

Figure S2

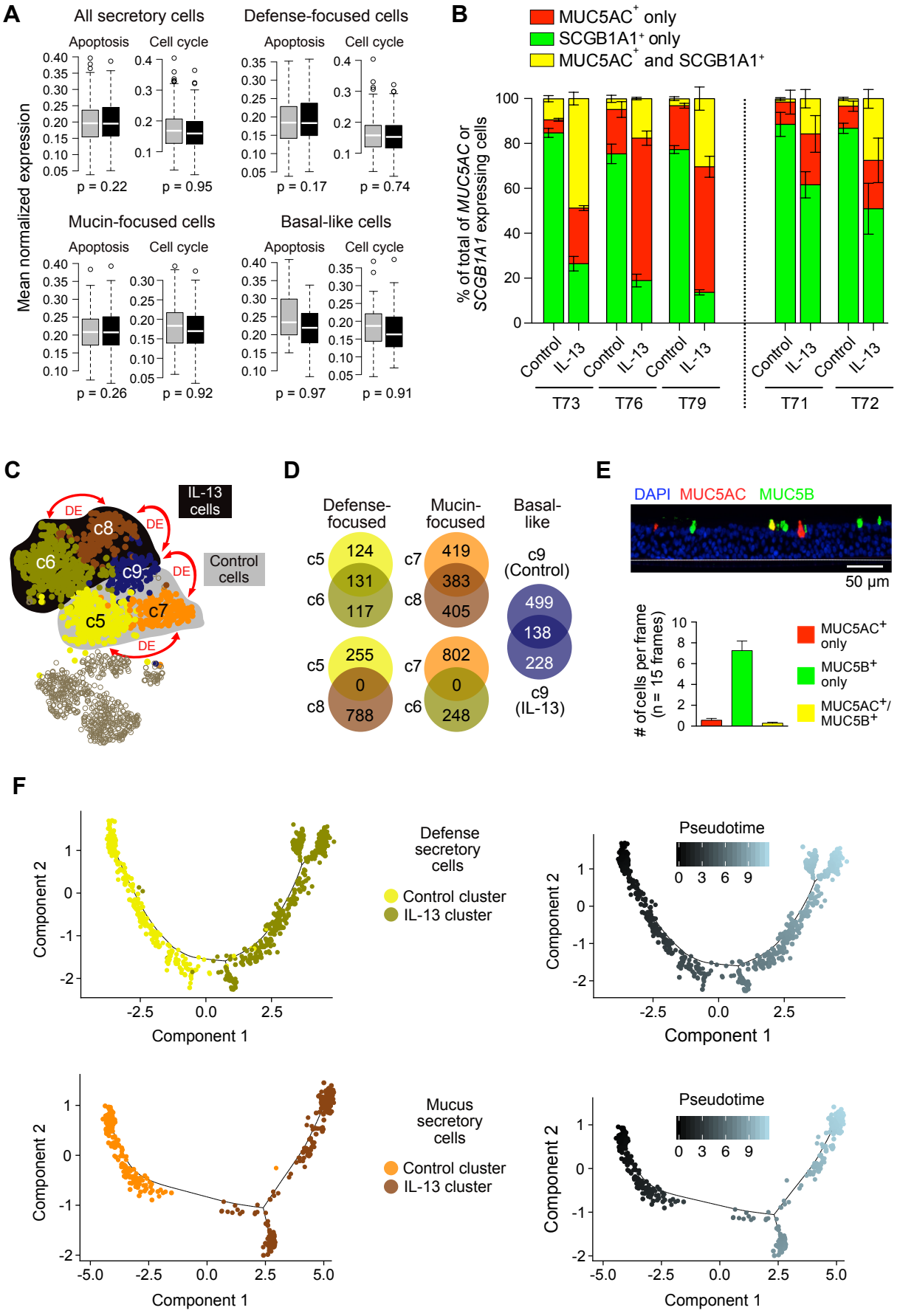
A
All secretory cells
Defense-focused cells
Mucin-focused cells
Basal-like cells
Apoptosis
Cell cycle
Mean normalized expression
p = 0.22
p = 0.95
p = 0.17
p = 0.74
p = 0.26
p = 0.92
p = 0.97
p = 0.91
B
MUC5AC+ only
SCGB1A1+ only
MUC5AC+ and SCGB1A1+
% of total of MUC5AC or SCGB1A1 expressing cells
Control
IL-13
T73
T76
T79
T71
T72
C
IL-13 cells
Control cells
DE
c8
c6
c9
c5
c7
D
Defense-focused
Mucin-focused
Basal-like
c5
c6
c7
c8
c9 (Control)
c9 (IL-13)
124
131
117
419
383
405
499
138
228
255
0
788
802
0
248
E
DAPI MUC5AC MUC5B
50 µm
# of cells per frame (n = 15 frames)
MUC5AC+ only
MUC5B+ only
MUC5AC+/ MUC5B+
F
Component 1
Component 2
Defense secretory cells
Control cluster
IL-13 cluster
Pseudotime
Mucus secretory cells

Figure S2 (related to Figure 3). Characterization of secretory cell populations in the *in vitro* airway epithelium

(A) Box plots showing that expression of genes annotated for Apoptosis or Cell cycle (KEGG pathways) was not increased by acute IL-13 stimulation in any of the secretory cell populations. P-values are based on one-sided Wilcoxon signed-rank tests.

(B) Related to Figure 3A. *Left*, Bar plots showing quantification of the average percentage of $MUC5AC^+$ only, $SCGB1A1^+$ only, and dual $MUC5AC^+/SCGB1A1^+$ cells relative to the total of MUC5AC and SCGB1A1-expressing cells across five top-down IF images for each of three HTEC donor cells (T73, T76, and T79) differentiated using ALI and then stimulated with IL-13 or BSA for 48 hours (acute stimulation). Average percentages across the three donors were 79.12% ($SCGB1A1^+$), 15.11% ($MUC5AC^+$), and 5.77% ($dual^+$) in the control (BSA) condition and 19.72% ($SCGB1A1^+$), 48.04% ($MUC5AC^+$), and 32.24% ($dual^+$) with IL-13. *Right*, similar IF quantification based on five top-down images and same magnification as in the left plots for the two tracheal donors used for scRNA-seq (T71 and T72).

(C) Description of differential expression (DE) analyses carried out to detect genes that define cell states within IL-13 and control-dominant secretory cell populations. tSNE plot and cluster assignments for secretory populations are as in Figure 2B. DE was performed between IL-13 cells in the IL-13-dominant secretory clusters, c6 and c8, and between control cells in control-dominant secretory clusters, c5 and c7. In addition, DE was performed between IL-13 cells in the basal-secretory cluster, c6, and the remaining IL-13-dominant clusters (c6 and c8 combined) as well as between control cells in c6 and the remaining control-dominant clusters (c5 and c7 combined).

(D) Venn diagrams depicting overlap of upregulated DEGs for each secretory and basal-like population, showing that c5 and c6 populations (and correspondingly, c7 and c8 populations) represent analogous cell states responding differently to control and IL-13 environments. Further supporting the c5 to c6 and c7 to c8 conversions, we observed similar frequencies of these population pairs (c5 [35%] and c6 [38%] versus c7 [23%] and c8 [22%]) within their respective control and IL-13 cultures.

(**E**) Immunofluorescence (IF) labeling of ALI-differentiated human AEC cultures stimulated with BSA for 48 hours (top) shows that, while difficult to detect transcriptionally, MUC5B is amply present and dominant over MUC5AC in baseline epithelia. Bar plots (bottom) showing quantification of the average percentage of $MUC5AC^+$ only, $MUC5B^+$ only, and dual $MUC5AC^+/MUC5B^+$ cells relative to the total of MUC5AC and MUC5B-expressing cells across IF images from two tracheal donors (T147 and T148) and 15 fields of view counted per sample.

(F) Monocle lineage trajectories for defense secretory (top) and mucus secretory cells (bottom), modeling the transition from baseline cells into those responding to an IL-13 environment. *Left*, cells colored by cluster identity; *Right*, cells colored by location along pseudotime.

Figure S3

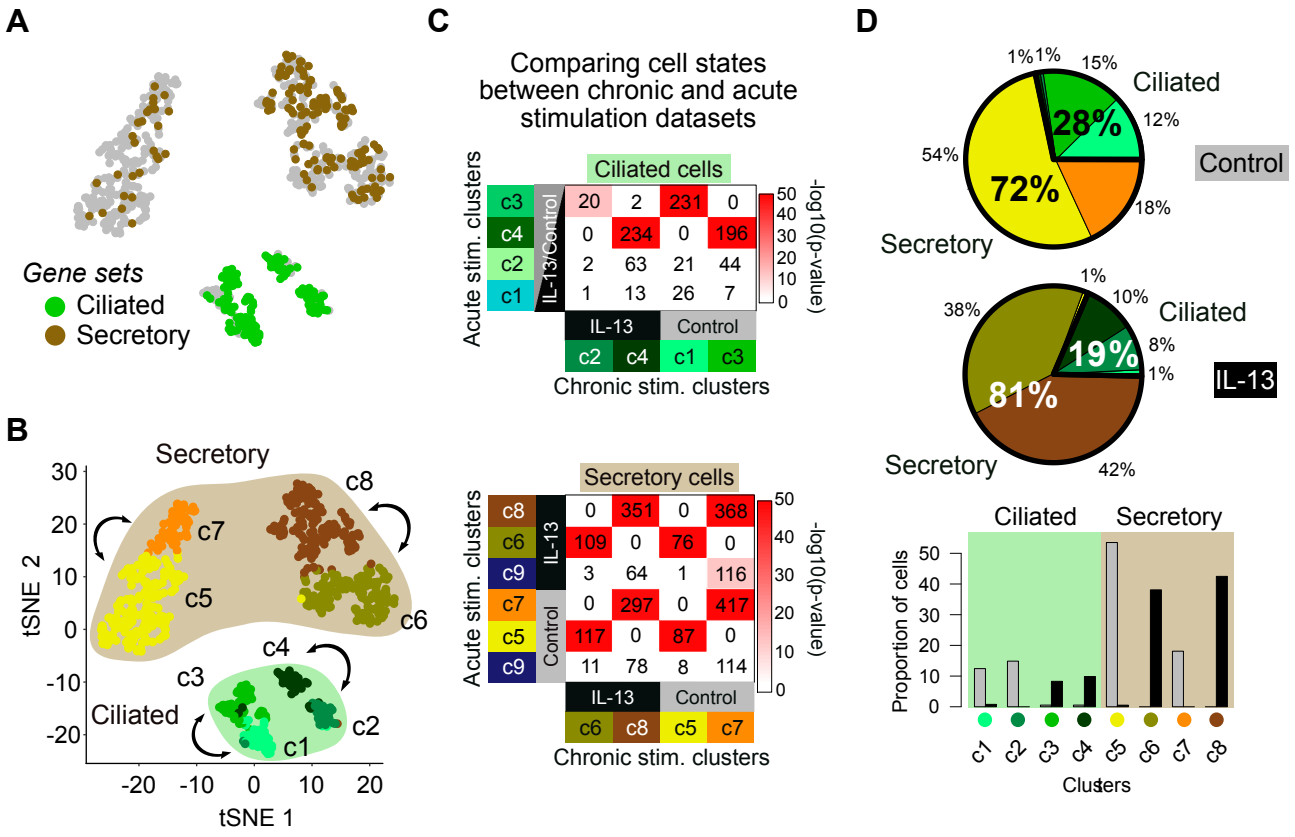
A
Gene sets
Ciliated
Secretory
B
Secretory
Ciliated
c1
c2
c3
c4
c5
c6
c7
c8
tSNE 1
tSNE 2
C
Comparing cell states between chronic and acute stimulation datasets
Ciliated cells
Acute stim. clusters
Chronic stim. clusters
IL-13
Control
-log10(p-value)
Secretory cells
D
Ciliated
Secretory
Control
IL-13
28%
72%
19%
81%
Proportion of cells
Clusters

Figure S3 (related to Figure 5). Characterizing single cell populations in the chronic stimulation dataset and comparing them with populations in the acute stimulation dataset

(A) Same tSNE plot as in Figure 5B, where cells are colored by whether they exhibit ciliated (green) or secretory (brown) cell gene signatures based on their mean expression of cell type-defining gene sets (the same sets used to define cells in the acute stimulation dataset; see Figure 2C).

(B) Same tSNE plot as in **A** showing clusters of the chronically stimulated dataset. Arrows identify populations compared in differential expression analyses to obtain cluster-specific gene signatures. These signatures were compared with signatures from analogous comparisons in the acute simulation dataset in **C**.

(C) Heat maps that illuminate analogous clusters between chronic and acute stimulation datasets. For ciliated cells (top) and secretory cells (bottom), degree of overlap between signature genes in acute dataset clusters and chronic dataset clusters is shown, revealing that cell states analogous to mature ciliated cell clusters (c3 and c4) and secretory cell clusters (c5 – c8) in the acute stimulation dataset can also be found in the chronic stimulation dataset.

(D) Pie charts (top) and bar plot (bottom) showing differences in the proportional distribution of cell types as well as cell states within each major cell group (ciliated and secretory) between control and IL-13-stimulated epithelia in the chronic stimulation dataset.

Figure S4

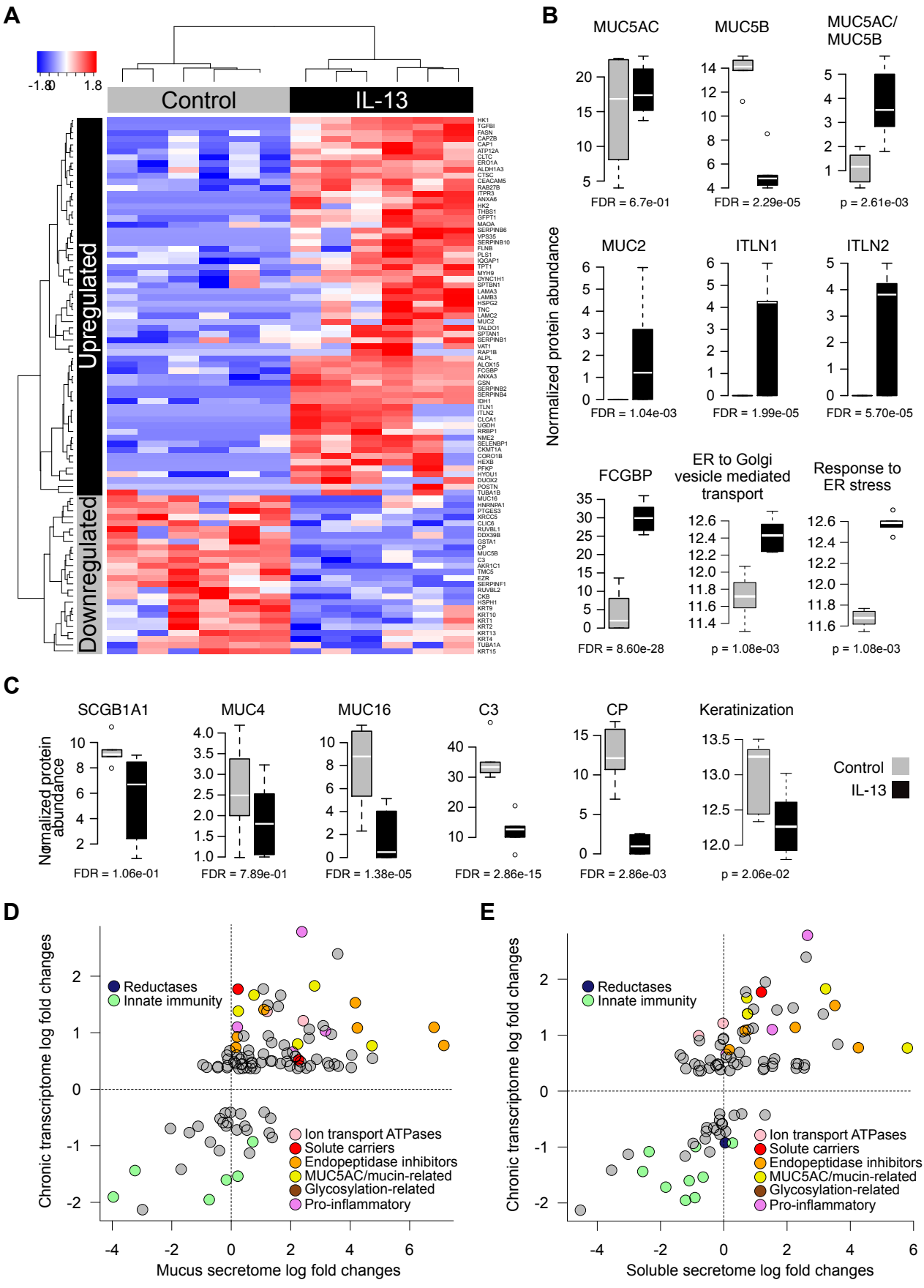
A
-1.8
0
1.8
Control
IL-13
Upregulated
Downregulated
B
MUC5AC
MUC5B
MUC5AC/
MUC5B
FDR = 6.7e-01
FDR = 2.29e-05
p = 2.61e-03
Normalized protein abundance
MUC2
ITLN1
ITLN2
FDR = 1.04e-03
FDR = 1.99e-05
FDR = 5.70e-05
FCGBP
ER to Golgi
vesicle mediated
transport
Response to
ER stress
FDR = 8.60e-28
p = 1.08e-03
p = 1.08e-03
C
SCGB1A1
MUC4
MUC16
C3
CP
Keratinization
Normalized protein abundance
FDR = 1.06e-01
FDR = 7.89e-01
FDR = 1.38e-05
FDR = 2.86e-15
FDR = 2.86e-03
p = 2.06e-02
Control
IL-13
D
Reductases
Innate immunity
Ion transport ATPases
Solute carriers
Endopeptidase inhibitors
MUC5AC/mucin-related
Glycosylation-related
Pro-inflammatory
Chronic transcriptome log fold changes
Mucus secretome log fold changes
E
Reductases
Innate immunity
Ion transport ATPases
Solute carriers
Endopeptidase inhibitors
MUC5AC/mucin-related
Glycosylation-related
Pro-inflammatory
Chronic transcriptome log fold changes
Soluble secretome log fold changes

Figure S4 (related to Figure 6). Effects of IL-13 on the insoluble (mucus) secretome are commensurate with those observed in the soluble secretome.
(A) Heat map of normalized spectral counts for apical secretome proteins from the insoluble (mucus) fraction that were significantly up- or downregulated with IL-13. Data based on paired HBECs from six donors.
(B) Box plots comparing mucus secretome protein abundance between control and IL-13-stimulated samples for proteins or enriched terms upregulated with IL-13. FDRs are based on DE analysis, p-values are based on one-sided Wilcox tests.
(C) Box plots comparing mucus secretome protein abundance between control and IL-13-stimulated samples for proteins or enriched terms downregulated with IL-13. FDRs are based on DE analysis, p-values are based on one-sided Wilcox tests.
(D) Scatter plot comparing the chronic transcriptomic secretory response to IL-13 with the apically secreted insoluble (mucus) protein response. Point coordinates are y = log fold changes in gene expression with IL-13 in secretory cells (clusters c5 – c9) in the chronic stimulation dataset and x = log fold changes in protein abundance with IL-13. All DEGs in the transcriptome dataset also in the secretome dataset are shown. Colored points refer to response molecules that are related to one of the specified function categories (same categories as in Figure 3C and Figure 4B).
(E) Scatter plot comparing the chronic transcriptomic secretory response to IL-13 with the apically secreted soluble protein response. Point coordinates are y = log fold changes in gene expression with IL-13 in secretory cells (clusters c5 – c9) in the chronic stimulation dataset and x = log fold changes in protein abundance with IL-13. All DEGs in the transcriptome dataset also in the secretome dataset are shown. Colored points refer to response molecules that are related to one of the specified function categories (same categories as in Figure 3C and Figure 4B).

Figure S5

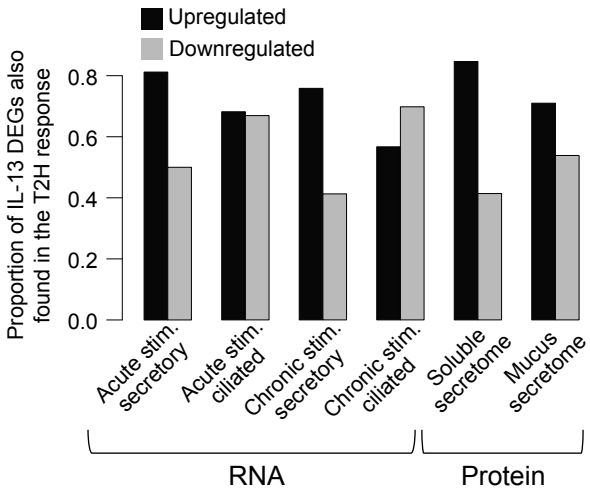
Upregulated
Downregulated
Proportion of IL-13 DEGs also found in the T2H response
0.0
0.2
0.4
0.6
0.8
Acute stim. secretory
Acute stim. ciliated
Chronic stim. secretory
Chronic stim. ciliated
Soluble secretome
Mucus secretome
RNA
Protein

Figure S5 (related to Figure 7). IL-13 responses observed using AEC cultures mirror secretory changes in the *in vivo* airway epithelium.
Bar plots showing overlap of the *in vitro* airway epithelial response, as observed in different cell types and datasets, and the response to T2 inflammation *in vivo*.

Table S1 (related to Figure 6). Summary results for fixed terms from linear mixed models that predict CBF as a function of IL-13 treatment (in pre- and post-washed datasets separately) or as a function of IL-13 treatment, wash status, and their interaction (in the combined dataset). Degrees of freedom (DF) and p-values are based on Satterthwaite approximations.

Variable	Estimate	Std. error	t value	DF (Satt)	p-value (Satt)
A. Top-down imaging					
Marginal pre-washed treatment effect					
Intercept	9.16	0.30	30.76	5.02	6.46E-07
Treatment (IL-13 compared to Control)	-2.15	0.03	-63.00	19671.98	<2.00E-16
Marginal post-washed treatment effect					
Intercept	9.50	0.52	18.33	5.02	8.62E-06
Treatment (IL-13 compared to Control)	-1.13	0.05	-21.90	17948.48	<2.00E-16
Combined pre- and post-washed treatment effects					
Intercept	9.18	0.37	25.14	5.04	1.71E-06
Treatment (IL-13 compared to BSA, pre-wash)	-2.19	0.04	-51.18	37624.60	<2.00E-16
Wash (post-wash compared to pre-wash, control)	0.32	0.04	8.12	37624.23	4.44E-16
Treatment:Wash (post-wash IL-13 shift compared to pre-wash IL-13 shift)	1.08	0.06	17.48	37624.26	<2.00E-16
B. Profile imaging					
Marginal pre-washed treatment effect					
Intercept	11.50	0.30	38.73	52.00	<2.00E-16
Treatment (IL-13 compared to Control)	-4.68	0.42	-11.15	52.00	<2.00E-16
Marginal post-washed treatment effect					
Intercept	10.71	0.47	22.81	1.54	6.26E-03
Treatment (IL-13 compared to Control)	0.84	0.54	1.54	33.01	1.32E-01
Combined pre- and post-washed treatment effects					
Intercept	11.56	0.36	31.78	3.36	2.74E-05
Treatment (IL-13 compared to BSA, pre-wash)	-4.68	0.42	-11.01	85.00	<2.00E-16
Wash (post-wash compared to pre-wash, control)	-0.87	0.45	-1.92	85.49	5.76E-02
Treatment:Wash (post-wash IL-13 shift compared to pre-wash IL-13 shift)	5.52	0.68	8.09	85.01	3.73E-12

Table S2 (related to STAR Methods). Description of tracheal sample donors.

	Donor 1 (T71)	Donor 2 (T72)
Age (years)	64	52
Sex	Female	Female
Smoking status	Former smoker (1pk/wk) x 3y	Current smoker (0.5 pk/d) x 40y
Disease status	No known diseases	Smoking-induced asthma (diagnosed 22 years prior)

Table S3 (related to STAR Methods). Description of bronchial sample donors. Note that the soluble apical samples are a subset of the insoluble apical samples. P-values are from t-tests for mean differences between subject classes.

Insoluble apical samples

	Control Subjects	Asthmatic Subjects	p-value
Sample Size	4	10	---
Age (years)	54.0 +/- 15.81	50.2 +/- 17.47	0.7132
Sex (% female)	75%	60.00%	0.5967
Smoker	0 / 4	0 / 10	---

Soluble apical samples

	Control Subjects	Asthmatic Subjects	p-value
Sample Size	3	3	---
Age (years)	60.33 +/-11.59	43.67 +/-26.10	0.3693
Sex (% female)	67%	33.30%	0.4142
Smoker	0 / 3	0 / 3	---

Table S4 (related to STAR Methods). Description of GALA II donors with RNA-seq data used in this study.

	Control Subjects	Asthmatic Subjects
Sample size	242	431
Sex (% female)	139 (57.4)	212 (49.0)
Age (years)	14.1 ± 3.1	14.0 ± 3.3
BMI (kg/m^2)	22.9 ± 5.3	24.3 ± 6.9
Total IgE (kU/L)	330.1 ± 566.7	521.3 ± 687.0
Eosinophils ($x10^3/\mu l$)	3.7 ± 2.9	4.9 ± 3.9
FeNO (ppb)	19.1 ± 16.2	30.5 ± 29.4
% FEV1	94.0 ± 13.7	88.2 ± 16.8

Table S5 (related to STAR Methods). Summary of single cell yield and mapping results, partitioned by experiment, chip, donor, and treatment.

Experiment	Chip	Donor	Treatment	N. lanes	N. cells	mean N. reads	mean N. UMIs	mean N. genes	mean % mapped	mean % mapped to genes	mean % mapped to mito genes
acute	91497	T71	BSA	3	256	392,394	7,163	2,411	79.03	69.48	7.18
acute	91497	T71	IL13	3	280	657,423	12,574	3,737	83.30	73.54	8.73
acute	91497	T72	BSA	3	250	514,443	9,982	3,100	82.60	73.34	9.11
acute	91497	T72	IL13	3	264	752,442	14,975	4,219	83.51	73.89	10.37
acute	94576	T71	BSA	3	324	420,146	8,622	2,960	84.96	74.43	6.56
acute	94576	T71	IL13	3	347	331,486	7,090	2,594	84.66	74.76	6.66
acute	94576	T72	BSA	3	330	340,246	7,309	2,636	84.78	74.93	7.57
acute	94576	T72	IL13	3	334	345,070	7,554	2,707	84.39	74.66	7.97
chronic	97570	T71	BSA	3	151	331,608	7,447	2,754	86.14	76.03	11.25
chronic	97570	T71	IL13	3	279	862,818	19,254	5,525	85.19	75.27	11.70
chronic	97570	T72	BSA	3	248	902,490	20,171	5,752	84.76	75.00	10.93
chronic	97570	T72	IL13	3	124	801,609	17,893	5,179	85.48	75.87	14.68